The effect of suspensions and racetrack three-dimensionality on the minimum lap time of motorcycles

Edoardo Marconi and Matteo Massaro*

Dept. of Industrial Engineering, University of Padova,
Via Venezia 1, 35131 Padova, Italy.
*matteo.massaro@unipd.it

Abstract. The aim of this work is to analyse the effect suspensions and the three-dimensional features of racetrack on the minimum-time performance of a full dynamic multibody model of a sports motorcycle. The optimal-control minimum-lap-time problem is solved with indirect methods on both a two-dimensional and a three-dimensional track model, and the results are compared. The effects of suspensions is also analysed.

Keywords: motorcycle dynamics, minimum-time problem, 3D road modelling, optimal control, free-trajectory

1 Introduction

The solution of optimal control problems (OCPs) for minimum-lap-time simulations have been applied to both two-wheeled and four-wheeled vehicles in the last decade [1]. Some examples of the application to race cars are [2–4], while in [5, 6] the optimal control of motorcycles is discussed. All of these works assume the track to be flat. This hypothesis constitutes in many cases a strong approximation of the real track geometry, and neglecting the three-dimensional (3D) features of the road can lead to inaccurate results. In [7–9] a 3D track model is used in the minimum-time optimal-control simulation of race cars. The literature dealing with the optimal control of a motorcycle riding on a 3D circuit only employs simplified motorcycle models [1, 10, 11].

In this work the effect of racetrack three-dimensionality on the lap time of motorcycles is investigated for a full motorcycle model. There are three main effects related to three-dimensionality.

1. The slope of the track induces a non-zero component of the gravity acceleration along the longitudinal axis of the vehicle, which sums with the accelerations related to the longitudinal controls of the vehicle (throttle and brakes). The related effect on the speed profile can be sensible.
2. The rate of change of the slope affects the tyre loads, e.g. when going over the brow of a hill the vehicle appears 'lighter'. Also in this case the effect on the acceleration and braking performance can be sensible.

3. The road banking angle has a strong effect on the cornering performance of the vehicle. Indeed, for a given lateral acceleration, a part of the centripetal force necessary to drive through the turn is generated from the tyre normal load, with a corresponding reduction in the required tyre lateral (tangential to the road) force. In addition, the increase in the normal load on tyre allows for a further increase in the achievable tyre tangential force. Again, significant effects are to be expected.

The minimum lap time of a nine degree-of-freedom full dynamic model of a sport motorcycle on a three-dimensional track is considered and solved through non-linear optimal control techniques. An indirect approach is chosen in this work [12]. The Mugello (Italy) race track is selected, see Fig. 1. Details about the track's geometry are reported in [11]. Moreover, in order to examine the effect of suspensions on the motorcycle's dynamic behaviour, the same model used to investigate the effect of 3D road features has also been simulated with locked suspensions.

Section 2 gives the essential characteristics about the vehicle model used. Section 3 describes the methodology employed for the solution of the minimum-lap-time problem. In Sec. 4 the effects of the three-dimensionality of the road on motorcycle dynamics are analysed. Section 5 highlights the effects related to the suspensions.

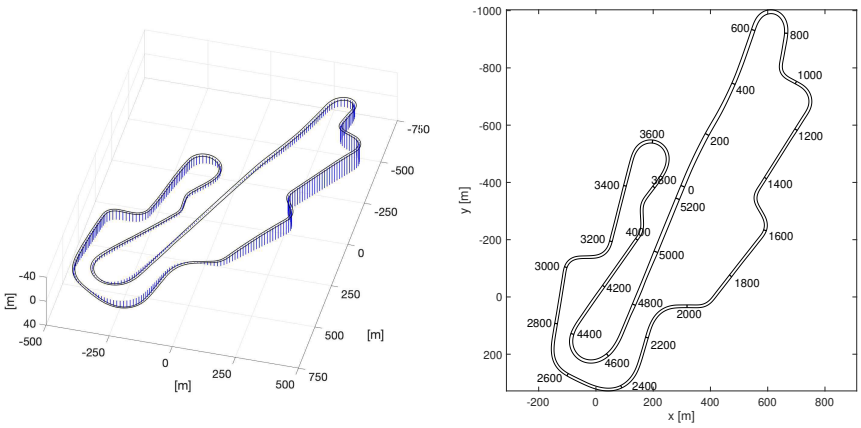

(a) (b)

Fig. 1: (a) Three-dimensional model of the Mugello circuit. (b) Planar view of the Mugello circuit with travelled distance (in metres) from the start/finish line.

2 Vehicle model

The vehicle model consists of the advanced non-linear multibody motorcycle model employed by the authors in [13], which has been extended to ride on three-dimensional roads. The model, developed using the Maple library MBSymba [14], consists of four bodies (main chassis with a rigidly attached rider, front frame, front and rear wheels) and nine degrees of freedom (chassis position and orientation, steering angle and suspension travels). The tyre model takes into account the shape of the crown radius (assumed toroidal). Steady-state lateral tyre forces depend linearly on the sideslip and camber angles and relaxation equations are included to account for the well-known 'lag' in the generation of tyre forces. The coupling between lateral and longitudinal forces is accounted for using friction ellipses. The position of the vehicle on the track is given by the travelled distance (i.e. curvilinear abscissa) along the road centreline, the lateral position with respect to the center line, and the relative orientation between the vehicle mid-plane and the tangent to the road center line. The vehicle dataset used in this study is reported in the appendix.

The road is modelled with 'ribbons' or strips, each one having an orientation given by three angles: heading θ, slope σ and banking β. The three related curvatures (κ, ν and τ), which are given as a function of the travelled distance from the start/finish line ζ, define the 3D track model, together with road width. Road curvatures and angles are linked by the following equations:

$$\kappa = \cos(\sigma)\cos(\beta)\theta' - \sin(\beta)\sigma' \tag{1}$$

$$\nu = \cos(\sigma)\sin(\beta)\theta' + \cos(\beta)\sigma' \tag{2}$$

$$\tau = -\sin(\sigma)\theta' + \beta' \tag{3}$$

where the dependence on ζ has been omitted and the prime symbol represents the derivative with respect to ζ. The reconstruction of the curvatures of the racetrack is obtained by solution of another optimal control problem, given the (x, y, z) coordinates of the left and right road borders, employing the methods reported in [1, 12]. In order to investigate the consequences of the 3D characteristics of the road, simulations are performed on both the full-feature track model and on a flat version of it. The latter is obtained by setting to zero the track's slope and banking angles, together with the corresponding curvatures. The two- and the three-dimensional track models share the same total travelled distance.

3 Optimal control

The non-linear OCP is solved adopting the indirect approach with implicit integration presented in [15]. Inequality constraints are added to the model, including maximum engine power, maximum steering angle and torque, maximum tyre friction (friction ellipse), maximum lateral distance from road centreline (road borders) and minimum tyre vertical loads (to avoid wheelie and stoppie). The constrained problem is transformed in an equivalent unconstrained problem using Lagrange multipliers and penalty functions. The optimal solution is

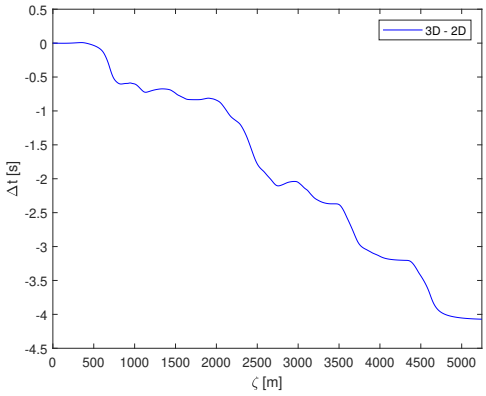

Fig. 2: Time gain of 3D vs. 2D, as a function of the curvilinear abscissa ζ.

found by solving a two-point boundary value problem (BVP), derived from the first variation of the unconstrained problem and discretised by finite differences. Symbolic calculations are used to evaluate the required derivatives for the BVP, as well as the associated adjoint equations. Due to the complexity of the motorcycle model here considered, the mass matrix cannot be inverted symbolically, and the solver must deal with the dynamics in implicit form.

4 Simulations: 3D effects

The main overall difference between the simulations performed on the two- and three-dimensional tracks is the lap time. The 3D simulation predicts a lap time of 106.030 s, while the lap time is 4.171 s longer in the case of the two-dimensional track. The time difference in built mainly in the U-turns at $\zeta = 700, 3600, 4500$ m, and in the section $\zeta = 2100 \div 2700$ m, see Fig. 2. These areas of the track present high banking angles in favour of the turn. The relative lap time difference (4%) is consistent with what has been found in [11], where a similar dataset is used, in conjunction with a simplified motorcycle model adopting MF tyres.

The 3D effects mentioned in Sec. 1 are studied analysing the dynamic behaviour of the vehicle in specific sections of the Mugello circuit, where they appear clearly.

4.1 Banking effect

The effect of banking is evident in the last turn of the circuit (*Bucine*, $\zeta = 4600 \div 4600$ m, see Fig. 1b). The essential dynamics in this turn are reported in Fig. 3. This is a U-turn with a maximum banking between 4 and 5 deg, where a distinctive double-apex trajectory is followed. When the banking angle is taken into account, the motorcycle is able to carry more speed into the turn, with an

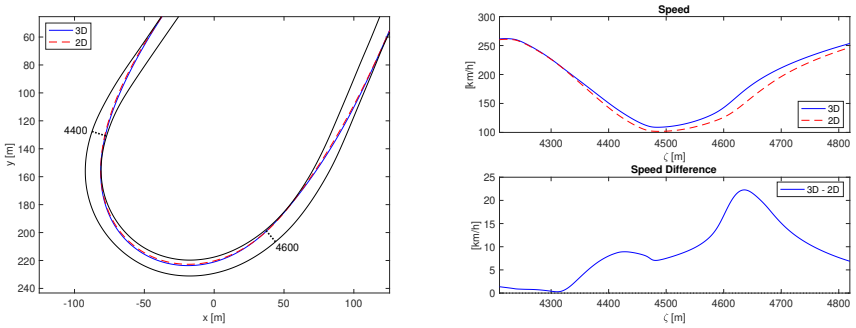

(a) (b)

Fig. 3: *Bucine* turn, 3D vs. 2D. (a) trajectory, (b) speed.

advantage of around 8 km/h between the two apexes. The high speed difference (above 20 km/h) at turn exit, again in favour of the 3D simulation, is due to an earlier (by roughly 25 m) application of the throttle. The total vertical tyre load and, consequently, the total lateral tyre force are roughly 10% larger in the three-dimensional case. The maximum camber angle (i.e. relative to the road plane) reached at $\zeta = 4500$ m is the same on both the two- and three-dimensional tracks. The maximum trajectory difference is found between the two apexes, in the middle of the turn, where the 3D simulation displays a trajectory 1 m wider. The 3D simulation is also tighter at turn entry and wider at the exit.

4.2 Slope and slope rate effect

The effect of the slope angle and the slope rate is noticeable in the straight at $\zeta = 2700 \div 3000$ m that follows the turns named *Arrabbiata 2* ($\zeta = 2600 \div 2700$ m, see Fig. 1b). Because of the effects described in the previous Sec. 4.1, the motorcycle on the 3D circuit exits from *Arrabbiata 2* with a speed advantage of around 10 km/h. The subsequent straight starts uphill (around 5 deg slope angle) and has a negative slope rate (around 0.03 deg/m). Because of the uphill slope, the acceleration of the motorcycle produced by the tyre longitudinal forces is opposed by the component of the gravity acceleration (of magnitude g) along the vehicle direction of travel, equal to $g\sin(\sigma)$. Moreover, the centrifugal effect connected to the negative slope rate makes the vehicle 'lighter', reducing the sum of the vertical loads on the two wheels. This causes the wheelie limit to be reached for lower longitudinal tyre forces (when compared to the flat track scenario). The combination of these two effects makes the motorcycle on the 3D track accelerate less out of *Arrabbiata 2*, sso that the speed advantage is reversed, with the two-dimensional simulation 7 km/h faster before braking to enter the next turn.

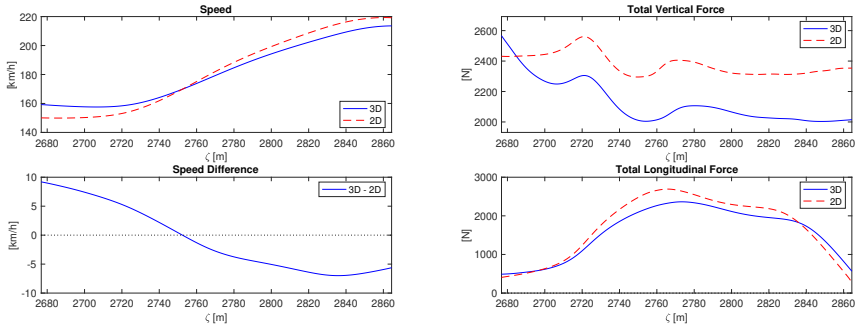

(a) (b)

Fig. 4: Straight following *Arrabbiata 2* turn: (a) speed, (b) total vertical and longitudinal tyre forces.

4.3 Remarks

Two additional simulations have been run in order to separate the effect of banking and slope. In the first simulation only the banking is included, while the slope is neglected. In more detail, the road track is reconstructed [1] using elevations of the left and right borders translated by their mean value. In the second simulation only the slope is included, while the banking is neglected. In this case, the road track is reconstructed using the same elevations for the left and right borders (equal to the mean of the actual elevations). It is found that the effect of banking is the most important: the lap time of the 3D track with the sole banking effect, i.e. without the slope, is 106.053 s, which is very close to 106.030 s obtained with the full 3D track model. On the contrary, the lap time of the 3D track with the sole slope effect is 109.933 s which is 3.903 s slower than the full 3D track model. Finally, these figures need be compared with 110.101 s, which is obtained with the 2D track. The effect of slope is visible on top speeds, with variations around 3 kph (full 3D vs. 3D with banking only). However, the main speed differences are in the middle of corners, and can reach 20 kph (full 3D vs. 2D).

5 Simulations: effects of suspensions

In order to examine the effect of the suspensions on the dynamic behaviour of the motorcycle, the simulation on the 3D track has also been carried out with locked suspensions. In this case, the only compliant parts of the vehicle model are the tyres, characterised by their normal stiffness and damping.

The lap time obtained with locked suspensions is 105.872 s, which is 0.157 s smaller than the one with free suspensions (0.15% difference). The time difference is built almost constantly over the lap (see Fig. 5), with the exception of the main

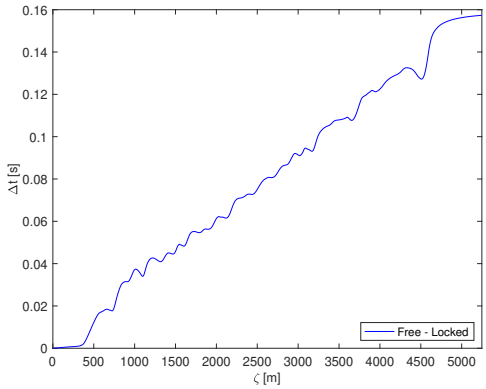

Fig. 5: Time gain of locked-suspension model with respect to free-suspension model, as a function of the curvilinear abscissa ζ.

straight, where the two models are substantially similar with respect to the lap time.

The maximum trajectory difference appears at $\zeta = 4550\,\mathrm{m}$, in the middle of the *Bucine* turn, where the locked-suspension model keeps a trajectory 0.28 m tighter.

Because of the lack of suspension travel, the locked-suspension model has a higher position of the centre of mass (differences up to 0.065 m mid corner), see Fig. 6a. As a result, the increment of the roll angle caused by the toroidal section of the tyre (with respect to the ideal case of lenticular tyres) is smaller in the case of locked suspensions. Indeed, the locked-suspension model reaches a maximum

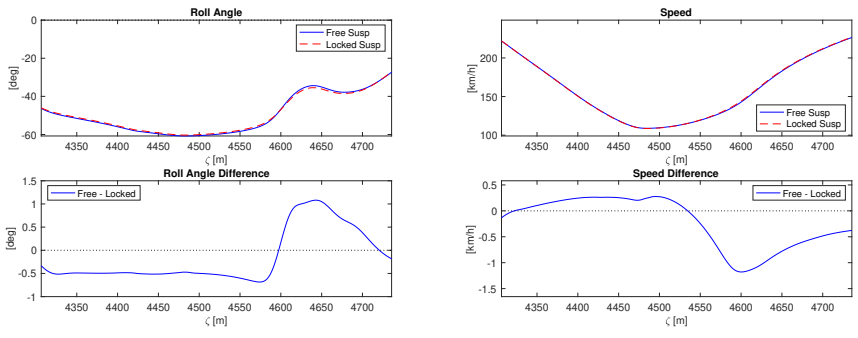

(a) (b)

Fig. 6: *Bucine* turn, free vs. locked suspensions. (a) roll angle, (b) speed.

camber angle of 60.3 deg, 0.6 deg smaller than that of the free-suspension model, which is consistent with analytical calculations [1, 16].

The small speed advantage, see Fig. 6b, of the model with suspensions on the middle of the *Bucine* turn is quickly reversed at the exit of the turn, since the locked-suspension model is able to accelerate slightly harder thanks to a higher load transfer towards the rear tyre while the maximum acceleration is friction limited. A similar behaviour is also observed at other turn exits.

6 Conclusions

The influence of the road three-dimensionality on the minimum lap time of a full motorcycle model (which includes the suspensions) has been studied. The effects of banking angle, slope angle and slope rate have been addressed, showing how much the behaviour of the motorcycle is affected. As for the lap time, the banking angle has proved the most influential 3D characteristic, at least in the case of the high-power motorcycle considered in this study. The main effect of slope and slope rate is related to the top speed in the straights. The differences highlighted are consistent with the outcomes found in the literature for simplified motorcycle models. The effects of the inclusion of the suspensions in the mathematical model of the vehicle have also been investigated, finding limited discrepancies between the full model and the one with no suspensions, with the current dataset.

References

1. Limebeer, D.J.N., Massaro, M.: Dynamics and optimal control of road vehicles. Oxford University Press (2018)
2. Hendrikx, J., Meijlink, T., Kriens, R.: Application of optimal control theory to inverse simulation of car handling. Vehicle System Dynamics 26(6), 449–461 (1996)
3. Casanova, D.: On minimum time vehicle manoeuvring: The theoretical optimal lap. Ph.D. thesis, Cranfield University (2000)
4. Perantoni, G., Limebeer, D.J.N.: Optimal control for a formula one car with variable parameters. Vehicle System Dynamics 52(5), 653–678 (2014)
5. Cossalter, V., Da Lio, M., Lot, R., Fabbri, L.: A general method for the evaluation of vehicle manoeuvrability with special emphasis on motorcycles. Vehicle System Dynamics 31, 113–135 (1999)
6. Bobbo, S., Cossalter, V., Massaro, M., Peretto, M.: Application of the optimal maneuver method for enhancing racing motorcycle performance. SAE International Journal of Passenger Cars-Mechanical Systems 1(1), 1311–1318 (2009)
7. Lot, R., Biral, F.: A curvilinear abscissa approach for the lap time optimization of racing vehicles. IFAC Proceedings Volumes 47(3), 7559–7565 (2014)
8. Perantoni, G., Limebeer, D.J.N.: Optimal control of a formula one car on a three-dimensional track – part 1: Track modeling and identification. Journal of Dynamic Systems, Measurement, and Control 137(5), 051018 (2015)
9. Limebeer, D.J.N., Perantoni, G.: Optimal control of a formula one car on a three-dimensional track – part 2: Optimal control. Journal of Dynamic Systems, Measurement, and Control 137(5), 051019 (2015)

10. Dal Bianco, N., Lot, R., Matthys, K.: Lap time simulation and design optimisation of a brushed dc electric motorcycle for the isle of man tt zero challenge. Vehicle System Dynamics 56(1), 27–54 (2018)
11. Leonelli, L., Limebeer, D.J.N.: Optimal control of a road racing motorcycle on a three-dimensional closed track. Vehicle System Dynamics pp. 1–25 (2019)
12. Dal Bianco, N., Bertolazzi, E., Biral, F., Massaro, M.: Comparison of direct and indirect methods for minimum lap time optimal control problems. Vehicle System Dynamics pp. 1–32 (2018)
13. Massaro, M., Marconi, E.: The effect of engine spin direction on the dynamics of powered two wheelers. Vehicle system dynamics 56(4), 604–620 (2018)
14. Lot, R., Massaro, M.: A symbolic approach to the multibody modeling of road vehicles. International Journal of Applied Mechanics 9(05), 1750068 (2017)
15. Bertolazzi, E., Biral, F., Da Lio, M.: Symbolic-numeric efficient solution of optimal control problems for multibody systems. Journal of computational and applied mathematics 185(2), 404–421 (2006)
16. Cossalter, V.: Motorcycle Dynamics. Lulu (2006)

Appendix

Table 1: Motorcycle (plus rider) dataset

Whole vehicle geometry and inertia	
Vehicle mass	250 kg
Height of centre of mass	0.70 m
Longitudinal distance of centre of mass from rear axle	0.73 m
Wheelbase	1.5 m
Normal trail	0.1 m
Caster angle	0.45 rad
Moment of inertia about the x-axis	18 kg m^2
Moment of inertia about the y-axis	50 kg m^2
Moment of inertia about the z-axis	40 kg m^2
Product of inertia ($I_{xz} = \int xzdm$)	-2 kg m^2
Front frame inertia	
Front frame mass	30 kg
Height of mass centre	0.55 m
Longitudinal distance of mass centre from rear axle	1.35 m
Moment of inertia about the z-axis (steer)	0.5 kg m^2
Aerodynemics	
Drag area coefficient (acceleration)	0.2 m^2
Drag area coefficient (deceleration)	0.5 m^2
Lift coefficient	0.05 m^2
Height of aerodynamic centre of pressure	0.51 m

Rear wheel and tyre	
Unsprung mass	25 kg
Spin inertia	0.65 kg m^2
Tyre radius	0.33 m
Tyre crown section radius	0.10 m
Tyre radial stiffness	150 kN/m
Tyre radial damping	200 Ns/m
Sideslip stiffness per unit load	15 rad^{-1}
Roll stiffness per unit load	0.8 rad^{-1}
Relaxation length	0.15 m
Longitudinal friction coefficient	1.3
Lateral friction coefficient	1.4
Front wheel and tyre	
Unsprung mass	10 kg
Spin inertia	0.40 kg m^2
Tyre radius	0.30 m
Tyre crown section radius	0.06 m
Tyre radial stiffness	150 kN/m
Tyre radial damping	200 Ns/m
Sideslip stiffness per unit load	13 rad^{-1}
Roll stiffness per unit load	0.9 rad^{-1}
Relaxation length	0.15 m
Longitudinal friction coefficient	1.3
Lateral friction coefficient	1.4
Suspensions	
Rear vertical stiffness	30 kN/m
Rear vertical damping	3.5 kNs/m
Front stiffness	30 kN/m
Front damping	3.5 kNs/m
Constraints	
Engine maximum power	145 kW
Maximum steering angle	0.2 rad
Maximum handlebar torque	200 Nm